Characterisation of porous solids using

small-angle scattering and NMR cryoporometry

J.C.Dore, J.B.W.Webber and J.H.Strange

[School of Physical Sciences, University of Kent, Canterbury, CT2 7NR, UK]

Keywords:
Mesoporous silicas, activated carbons, small-angle scattering, cryoporometry, neutron diffraction

Abstract
The characteristics of several porous systems have been studied by the use of small-angle neutron scattering [SANS] and nuclear magnetic resonance [NMR] techniques. The measurements reveal different characteristics for sol-gel silicas, activated carbons and ordered mesoporous silicas of the MCM and SBA type. Good agreement is obtained between gas adsorption measurements and the NMR and SANS results for pore sizes above 10 nm. Recent measurements of the water/ice phase transformation in SBA silicas by neutron diffraction are also presented and indicate a complex relationship that will require more detailed treatment in terms of the possible effects of microporosity in the silica substrate. The complementarity of the different methods is emphasised and there is brief discussion of issues related to possible future developments.

1. Introduction

Porous solids occur naturally in a mineralogical or biosciences context but the main interest is in fabricated materials for use in industrial processes. Furthermore, the properties of solids and liquids confined inside the pores are significantly modified in terms of thermophysical, structural and electronic properties.

The earliest forms of porous material were based on carbon and there is continued interest in the properties of activated carbons and, more recently, carbon nanotubes. However, the most useful material for research purposes in the mesoporous range has been silica, which can be used to produce well-characterised mesoporous solids with controlled characteristics. Another material with specific properties is alumina, fabricated in the form of an anodic membrane.

2. Characteristics of porous materials

The main advantage of mesoporous materials is the high internal surface area, which is exposed to any liquid, gas or vapour phase. Specific surface interactions occur, due to interfacial forces, that lead to a modified behaviour compared with the bulk phase. This feature is used in heterogeneous catalysis but there are other properties that are of interest and depend on the modified phases of the adsorbed/confined material.

The most basic property is the distribution function for the mean pore sizes. Some materials have a very narrow pore size distribution (~10%) and are regarded as ‘monodisperse’ but others may have a very wide range, spanning the micro-pore to macro-pore regions. The pore network is also of importance and may be disordered or ordered. The sol-gel process leads to a disordered pore volume but the overall system does contain structural features. In contrast, a templating process is used to produce the MCM- and SBA-silicas and the resulting networks have a well-defined lattice structure on a mesoscopic scale. Similarly, the anodic aluminium oxide [AAO] membranes have a strongly-

oriented set of identical parallel cylindrical pores that have larger diameters than the MCM/SBA silicas.

3. Experimental techniques

a) Small angle scattering

Small angle scattering of x-rays and thermal neutrons provides a direct measurement of spatial inhomogeneities in the sample material.

For the porous materials comprising a solid matrix with a pore distribution represented by $\rho(\mathbf{r})$, the scattering intensity $I(\mathbf{Q})$ may be written in general form [1] as:-

$$I(\mathbf{Q}) \;=\; K \left| \int \rho(\mathbf{r}) \exp(i\,\mathbf{Q}.\mathbf{r})\, d^3\mathbf{r} \right|^2, \qquad (1)$$

where K is a normalisation constant and $\mathbf{Q}$ is the scattering vector. For a two component system of pores and voids with a homogeneous solid phase density of ρ_S, the expression is freqently written, in terms of a distribution of defined 'particles' or pores, by separating the two spatial components. The approximate expression for a dilute system then becomes:-

$$I(Q) \;=\; K\, \rho_S^2\, S(Q) \left| F(Q,R) \right|^2, \qquad (2)$$

where $F(Q,R)$ is a form-factor that characterises the distribution of pore sizes and shapes and $S(Q)$ is a structure factor that represents the spatial distribution of the pores.

An alternative approach to the description of spatial features involves the use of correlation functions that are more familiar in the description of the atomic pair distribution function for disordered materials such as glasses and liquids. In the SAS regime, the summation over individual atom sites becomes an integral over the inhomogeneous density distribution, such that a spatial correlation function can be evaluated from the transform relation [2] :-

$$d(r) \;=\; r.G_\rho(r) \;=\; 4\pi r\,[\rho(r) - \rho_\infty] \;=\; \frac{2}{\pi} \int_0^\infty Q[S(Q) - S_\infty] \sin Qr\, dQ\,, \qquad (3)$$

This expression only assumes that there is a random orientation of the pore shapes and sizes throughout the sample material (i.e. no anisotropy). The transformation procedure is routinely used in the analysis of disordered materials, and is clearly model-independent; it just converts the experimental observations (as a function of Q) to a corresponding spatial distribution (as a function of r). Both functions may be used as a basis for further analysis using specific models of the pore structure.

To obtain a more detailed understanding of the pore characteristics, the correlation function approach has been used by various workers, while others now use chordal descriptors, [3-10]. However, the G(r) or d(r) curves do not relate simply to a pore size distribution function as determined by techniques such as gas adsorption, unless certain assumptions are made concerning pore shapes and size variations.

Typical values of Q for instruments devoted to small-angle scattering are 10^{-3} - 0.2 Å^{-1} for neutrons and 5.10^{-5} - 0.2 Å^{-1} for x-rays, covering a spatial range of ~1nm - 1μm. Conventional systems use a monochromatic incident beam with an area multidetector that is usually moveable to select the Q-range appropriate for the experiment. The complete 2D intensity profile is measured so that any anisotropy resulting from orientational effects in the sample material is immediately apparent.

The SAS method has been widely developed and there is a large literature on instrumentation and analysis procedures. The main limitation to the method is in devising a suitable analytic form for *F(Q,R)* with meaningful parameters and it is frequently necessary to make approximations in the data fitting process, particularly where there is a high porosity. The alternative approach for the 'non-dilute' systems studied here, is to create models of the nanoporous systems, and then to perform direct analytic and numerical evaluation of the solid-solid radial distribution function *G(r)* and thus the corresponding *I(Q)*, for comparison with the measured scattering [9, 10]. This method offers many advantages in practice, and is discussed further for the particular case of sol-gel silicas in Sec.4a.

b) NMR Cryoporometry

A particularly powerful set of techniques used to study mesoscopic structures involves imbibing a liquid into a porous media, and then investigating the physical properties of the confined phases. One of these techniques uses the Gibbs-Thomson equation [11], which relates the depression in the melting temperature to the pore dimensions, and is routinely used in differential scanning calorimetry [DSC] or thermoporosimetry [12].

The Gibbs-Thomson equation for the melting point depression ΔT_m for a small crystal of diameter x is given by :-

$$\Delta T_m = T_m - T_m(x) = \frac{4\sigma_{sl} T_m}{x \Delta H_f \rho_s} \tag{4a}$$

where T_m is the normal melting point of the liquid $T_m(x)$ is the melting point for crystallites of diameter x, σ_{sf} is the surface energy at the liquid-solid interface, ΔH_f is the bulk enthalpy of fusion (per gram of material) and ρ_s is the density of the solid., which may be rewritten as:-

$$\Delta T_m = \frac{k_{GT}}{x} \tag{4b}$$

The Gibbs-Thomson equation is the constant pressure (varying temperature) analogue of the constant temperature (varying pressure) Kelvin equation.

A variant of the usual thermoporisimetry technique, termed NMR cryoporometry [9,10,13-16] has been developed, using nuclear magnetic resonance to determine the quantity of liquid inside the available pore volume. The sample is cooled so that all the liquid in the pores is frozen and the material is then heated slowly (typically at a rate of 0.2 $K.min^{-1}$). The magnitude of the NMR signal from the mobile protons in the liquid state is measured as it develops during the warming process. Fig, 1a shows a typical curve for an over-filled sample of cyclohexane in a sol-gel silica. The curve has a plateau region where the absorbate has completely melted and a further rise that occurs at the normal bulk melting point [6.5^o C] due to the excess liquid on the outside of the grains. The pore distribution function may be determined directly from this melting curve using the Gibbs-Thomson expression (4), with a suitable calibration constant k_{GT}, and the resulting function is shown in Fig. 1b.

The NMR method has a number of advantages over the DSC method since the measured signal does not rely on transient thermal flows but measures the quantity of liquid directly. Consequently, the temperature ramp can be adjusted to fit the conditions of the material under investigation and a well-defined pore size with a sharp transition can be studied with a slower temperature variation. The method is conveniently used over a length scale extending from 2nm to 2μm. Comparative studies on sol-gel materials (Sec.4a) have shown that there is good agreement between DSC, gas adsorption and NMR cryoporometry over the range 2nm to 50 nm [9,10] (Fig. 2).

NMR cryoporometry can also be combined with standard NMR imaging techniques to give spatial resolution in one, two and three dimensions on a macroscopic scale [14]. Fig. 3 shows the two-dimensional case of four 4mm internal diameter tubes containing powder samples of sol-gel silicas with different pore diameter. Each of the tubes is clearly resolved and the corresponding pore characteristics are simultaneously identified. NMR cryoporometry is probably the only method currently capable of resolving the 3D bulk macroscopic distribution of a nano- or meso-structured porous material on a 100μm to 10mm length scale and currently has applications in geological and biological studies, as well as material studies for the construction industry.

c) Comparative studies and complementarity

Much of the investigation of pore characteristics is commonly conducted by gas adsorption measurements (as represented at this meeting). The main objective is to determine the pore size distribution function, $P(r)$, pore volume, V_P, and surface area A_S, which can be used for applications involving condensed phases in the pores. When different sample materials are fabricated, it is usually a relative evaluation that is required and a detailed quantitative determination of the 'real' pore distribution characteristics is not usually required. However, a related question arises as to whether the different techniques produce the same values for the defining parameters. Since the various methods rely on different physical assumptions, it is not obvious that the results will necessarily be equivalent. For example, mercury injection porosimetry is commonly used and determines the pore throat diameter as opposed to the mean pore diameter.

A comparative investigation of measurements inter-relating data from gas adsorption, DSC thermoporosimetry, NMR cryoporometry, NMR relaxation, NMR relaxometry, NMR diffusion, neutron diffraction and small angle neutron scattering measurements on a standard set of materials has therefore been instituted, in addition to the use of density and imbibation techniques [9,10,16]. Preliminary critiques of the results obtained from the different techniques have been published elsewhere [16], but some general remarks are made in Section 4.

Furthermore, considerable progress has been made in the representation of sol-gel silicas by creating analytic and numerical models of extended arrays of pore structures that can be directly compared with the experimental data. Such methods are related to the work of Stepanek et al [17] and Levitz [18] as presented at this meeting and discussed in Sec 4a. The complementarity of the different methods is apparent and a suitable combination of the information should be capable of revealing characteristics that no single technique can give on its own [16].

4. Example mesoporous materials

a) Sol-gel silicas

Mesoporous silicas can have a wide range of characteristics. We have studied samples of sol-gel silicas, covering a range of 2.5 to 50 nm in median pore size, prepared by several commercial companies. Gas adsorption, neutron diffraction, SANS and NMR cryoporometry with confined water or cyclohexane have been used in an extensive investigation of these materials. Small-angle neutron scattering experiments were made at the Institut Laue-Langevin, Grenoble with the D22 instrument and corresponding diffraction measurements used the D4B or D20 diffractometers. The combined SAS/diffraction results on the dry samples are shown as a *log[I(Q)]* vs. *log[Q]* plot in Fig 4 and cover a total Q-range of ~10^{-3} to 17 $Å^{-1}$ [9,10]. The low-Q region shows a strong SAS signal with a structure factor peak that changes position with the pore size and is typical of sol-gel silicas; the peak position is inversely related to the pore size. The diffraction region, at higher Q-values, gives information on the composite pair correlation function for silicon and oxygen atoms in the network glass, and on the incoherent scattering, but will not be discussed here.

Interpretation of the SAS data has often been through the use of eqn. 2 with a form-factor for spheres, coupled to a defined polydispersity function, but recently a range of approaches have been discussed [3-10]. One method is to combine the scattering results with those from other measurements to constrain a set of parameters that can be used to generate a model of extended arrays of randomised pores, to represent the basic structure of an idealised dry sol-gel silica. The NMR cryoporometry data suggests that a Gaussian variance is more appropriate for these sol-gel silicas than a fractal description [10]. The voids may be modelled as spheres with varying spacing and varying diameter. The model includes parameters for the grain density, the voidless silica density, the pore diameter, the 'lattice' spacing and their associated variances [9-10].

A Monte-Carlo integration routine is then used to calculate the expected solid-solid radial correlation function *G(r)* for these extended randomised structures of model pores, and hence the scattering intensity *I(Q)* from the Fourier inverse of eqn 3. The *G(r)* curves as measured for the seven silicas are compared in Fig. 5, with those calculated by this method; the two curves are superimposed and cannot be distinguished on this scale. Consequently, there is good overall agreement in the results obtained from a combination of data from gas adsorption, SANS, NMR cryoporometry, density and imbibation measurements. The experimental *G(r)* function is a one-dimensional spatial correlation function that represents an orientational average over the pore network and can itself be used for modelling in three-dimensions using various reconstruction procedures. However, it is usually more convenient, as in this case, to start with a suitably parameterised model and to optimise the model to fit the observations.

This work on dry silicas is currently being further extended using analytic and numerical models to aid the interpretation of combined NMR, SANS and diffraction studies for fully and partially liquid-filled silicas. The aim is to extend the investigation to liquid-surface interactions in these systems and to distinguish the effects of wetting and non-wetting conditions.

b) Carbons

A comprehensive review of small-angle scattering by carbons has been produced by Hoinkis [19] in 2000 for a wide range of carbonaceous materials. The results emphasise the difficulties of reaching unambiguous conclusions for these highly complex materials that have a very wide range of pore sizes and ribbon-like structures based on distorted graphene sheets.

The activated carbons represent an interesting subset and are formed by pyrolysis in an oxygen-free atmosphere of organic or synthetic materials. Gas adsorption measurements show that the

pore structure is complex and covers a wide range of sizes. The commercially available BP-carbons have formed the basis for a detailed evaluation of gas adsorption data by Quirke, Walton and collaborators [20] using density functional theory and a slit geometry to represent the pores. Gardner et al. [21] reported a series of SAXS measurements on the same materials and used several different approximations to model the data.

A full set of data is shown in Fig. 6, combining USAXS, SAXS and pulsed neutron diffraction measurements. In order to obtain fits to the SAXS results, it was found necessary to introduce a fractal term into the form-factor and even then, the fit showed systematic discrepancies. The use of a specific slit form-factor with the size parameters extracted from the gas adsorption data was clearly inadequate in representing the experimental data. This outcome clearly demonstrates the problems that may result in comparing the results from different techniques. The SAXS data are sensitive to the shapes of the pores and demonstrate that the current model used in the interpretation of the gas phase data is inaccurate. However, the SAXS data are insufficient to show how a more refined description of the pore network could lead to a reconciled model that would explain all the measurements. The diffraction data show that the atomic correlations can be explained on the basis of a paracrystalline formalism [22] based on short-range correlations between and in the graphene sheets. It also seems likely that the sheets are not planar [23], which may explain the high level of microporosity. Consequently, it is clear from the combination of different experimental methods that the current models are too simplified. Further work on the process of structural reconstruction from the various experimental observations is being undertaken by Pellenq and colleagues and it is hoped that a clearer understanding of the pore morphology will emerge from this study.

c) MCM and SBA silicas

Ordered mesoscopic silicas can be produced by a templating process using organic molecules that are subsequently removed by calcining. The first class of materials fabricated by this method was the MCM series with cylindrical-shaped pores of typically 25-35 Å diameter. The most common types are MCM41 consisting of a parallel hexagonal lattice of parallel pores and MCM48, which consists of a branched network of interconnected pores. More recently, the SBA-15 series has been developed with larger pores of 60-100 Å diameter arranged in parallel form similar to MCM41. In these cases it would seem that the pore characteristics are effectively defined by the geometrical structure and the only relevant parameter is the pore diameter. However, it is found that the quality of the fabricated SBA-15 materials can be variable and there is a microporous component that is difficult to fully quantify [24].

One of the features of the MCM silicas is the large depression of nucleation temperature arising from the small pore size. Neutron diffraction studies [25] have shown that liquid water can be cooled to 45K below the normal bulk freezing point before nucleation to a defective form of cubic ice. DSC and NMR cryoporometry measurements confirm the deep under-cooling. but the large fraction of the pore volume that is in close proximity to a silica surface does not necessarily lead to a simple interpretation using the Gibbs-Thomson equation.

Findenegg and colleagues [26] have reported a comprehensive series of measurements for water in both MCM and SBA silicas of varying pore size, using gas adsorption, DSC and SAXS. An interesting feature occurs for the partially-filled case of water in SBA silicas of 60 Å diameter, where the DSC data reveals two separated peaks, suggesting the possibility of two pore networks. However, recent neutron diffraction results suggest that this behaviour may be due to separate nucleation and growth events within the same pore structure. Further support for this behaviour has also recently been obtained from corresponding NMR measurements over the same

temperature range, which show that the confined water/ice exhibits a higher mobility than would normally be expected for pure ice, in agreement with earlier work on sol-gel silicas [27,28]. It now seems that the phase relations for water and ice in confined geometry are more complex than previously thought and more studies will be required to fully understand the processes. Temperature variation studies over a wide range suggest that the structure and dynamics display continuous change well below the onset of nucleation. The role of defective cubic ice in this context is still rather puzzling and the high proton mobility may possibly be attributed either to proton hopping in the solid phase or rotational motion in the 'disordered' layer at the interface. However, an alternative explanation is feasible if there is a significant quantity of water in a microporous environment and consequently, a detailed evaluation of the pore characteristics will be required to obtain an unambiguous interpretation of the data.

The neutron diffraction pattern for D_2O water in SBA silica of 92 Å pore diameter at various temperatures is shown in Fig. 7 for an over-filled sample. Previous work on ice nucleation in the sol-gel and MCM silicas has been published earlier [29,30], displaying the characteristic triplet peak of ice I_h and the asymmetric peak profile for ice I_c in the range 1.5-2.0 $Å^{-1}$. These features are reproduced in the study of water transformation in the SBA silica, where the separate components can be attributed to water on the outside of the grains [I_h] and the confined water [I_c]. This distinction allows a similar analysis to the DSC and NMR cryoporometry measurements; a more detailed paper on 'neutron diffraction cryoporometry', relating phase and pore structure, is in preparation.

5. Discussion

The above sections have reviewed a number of inter-related themes in the study of porous materials by different techniques. It seems clear that, where information of a comparative nature is required, a single method of investigation with suitable parameter fitting routines is adequate. However a more detailed understanding of the 'real' pore structure in terms of spatial correlation functions poses a much more fundamental problem in terms of the models used for its representation. The three types of material used in this review, namely sol-gel silicas, activated carbons and MCM/SBA silicas have quite different characteristics and pose distinct problems.

a) Sol-gel silicas
   Considerable effort has been expended on the characterisation of sol-gel silicas, often using a distribution of spheres or cylinders as the most convenient representation. However, the actual material is expected to be much more disordered in terms of the shapes and structures of the void volume and requires a larger number of parameters to give a realistic description of its variability.
b) Carbons
   The activated carbons form a large class of materials with quite different characteristics. They are clearly of a complex structure based on curved graphene sheets of varying thickness, width and separation. A satisfactory model for the interpretation of the data does not seem to exist and it will be necessary to combine the results of several techniques together to obtain a definitive solution. The micropores extend down to dimensions of <10 Å, which is comparable with the mean separation of the graphene sheets at 3.3-3.5 Å. In this context, the variation of the intra and inter-atomic correlations will be relevant to the distortion of the sheets and the creation of the micropore volume.
c) Ordered silicas
   The ordered silicas, of MCM and SBA type offer the most obvious possibilities for further development due to the regular nature of the pore network. The well-defined geometry and the

high aspect ratio of the cylindrical pores should enable detailed molecular dynamics calculations to be conducted to give a quantitative basis to the data treatment. The most recent results seem to suggest that the constant used for water in the Gibbs-Thomson equation may be different for the sol-gel and MCM/SBA systems. Since the ordered silicas have a well-defined geometry, this recent finding implies that the calibration constant should be treated as a shape-dependent parameter [15]. However, the use of water/ice is a natural choice for the confined absorbate. The latest studies have revealed unexpected complications, which are interesting for the study of hydrogen-bond interactions and networks but do not necessarily provide a clear interpretative picture for the characterisation of the pore structure. The alternative use of cyclohexane [9,10,15,16,31-33] may be feasible but the very high magnitude of the freezing point depression in these small pores creates other problems. The SAS method readily yields the lattice structure for the distribution of pore centres but needs a model to provide information on the pore size and its distribution.

d) Complementary methods

The previous sections have emphasised the way in which various experimental observations can be used to extract information on the characteristics of mesoporous materials. It has been shown that all techniques are valuable in providing comparative data using idealised models for the pore distribution but that details of the 'real' structure are profoundly difficult to isolate except possibly in the case of well-defined geometrical networks. Another method that can be used to determine pore sizes and shapes is positron annihilation [34], using the ratio of two- and three-photon decay processes to distinguish spatial features. It seems likely that this relatively under-developed technique will also play a role on future studies.

6. Summary and future work

The detailed and fundamental characterisation of pore structures by experimental methods poses many conceptual and interpretative problems that have not yet been adequately solved. Although chosen model descriptions can be readily applied to extract parameter values from the observations, a full determination of the spatial correlations is rarely feasible. There are, now, many possible experimental methods that rely on various assumptions. They can be classified into six main groups depending on

- adsorption isotherms [gas adsorption, Kelvin equation],
- melting point depression [thermoporosimetry, cryoporometry, Gibbs-Thomson equation],
- surface-liquid interaction [NMR relaxation, NMR relaxometry, NMR spin diffusion]
- coherent interference [neutron and x-ray scattering]
- liquid diffusion/mobility [NMR magnetic field gradient methods],
- direct imaging [microscopy/tomography, AFM, NMR microscopy/imaging[35]].

Pore connectivity is an important parameter that is less easily investigated unless some fluid transport property is determined.

At present, there are only partial attempts in the literature to cross correlate the information obtained from different techniques. It would be of considerable interest to take a standard material and to subject it to all the currently available methods and then to compare the extracted results. This approach would isolate the individual features of each method and give a greater insight into the accuracy of the individual techniques, with the additional possibility that the supporting theoretical basis could be confirmed or refined. The three classes of materials discussed in Sec, 3 would probably lead to different criteria in this evaluation process as they each emphasise different

characteristics, and the surface-liquid interactions in the carbons are very different from those in the silicas. It may be that the MCM and SBA systems offer the most direct prospects as they are thought to have well-defined geometry.

Another development concerns the interest in smaller pores. Considerable work has been presented over many decades for zeolites but there is now an additional interest in the adsorption/encapsulation of materials in carbon nanotubes. Gas adsorption in carbons offers great opportunities for hydrogen and methane storage but there are also interests in the thermophysical and electronic properties of the confined materials. Typical measurements by Kaneko et al [36] for various gases in carbon nanohorns indicate the type of investigation that can be conducted. Zeng and co-workers [37] have predicted that a new form of pentagonal ice may be created in the nanotubes and some preliminary x-ray studies have been made [38]; neutron studies are already planned [39].

7. Conclusions

Various experimental techniques are now available for the study of pore characteristics, but it is clear that the extraction of specific information is often based on theoretical assumptions that may be untested, or mathematical approximations to the representation of the essential structural features.

Although comparative measurements for different sample materials can be made using a single experimental technique, it is becoming increasingly clear that a realistic modelling of the pore network in general terms will require a more precise syntheses of various experimental investigations, coupled to extensive computer modelling. This development is now feasible and effectively defines a new phase for the continuing and evolving interest in porous solids and the materials confined within them. The examples given here are chosen to illustrate the diversity of issues that will need to be addressed as the subject progresses.

8. Acknowledgements

The work presented in this paper is drawn from an extended series of measurements covering the last five years. We would like to acknowledge many people who have contributed to the broad range of the investigation, with a particular mention of Ashley North, Michelle Gardner, Lee Betteridge [all Kent], Andrzej Burian [Katowice] and, more recently, Gerhard Findenegg [Berlin] (concerning the ongoing SBA studies). The work has been supported in various ways by EPSRC through grants and beamtime allocations.

References

1) L.A. Feigin and D.I. Svergun. Plenum Press, `*Structure Analysis by Small-Angle X-Ray and Neutron Scattering*', New York, (1987).
2) P. Chieux, J.C. Dore, p. 101 in `*Hydrogen-bonded liquids'*, vol 329: Mathematical and Physical Sciences ASI Series, Kluwer (pub), (1989).
3) B. Smarsly, K.Yu, C.J. Brinker. Stud. Surf. Sci. Catal. 146: (2003) 295-298.
4) E.S. Kikkinides, K.L. Stefanopoulos, T.A. Steriotis, et al. Appl. Phys. A-mater. 74: Part 2 Suppl. S (2002) S954-S956.
5) W. Gille, O. Kabisch, S. Reichl, et al. Micropor. Mesopor. Mat. 54 (1-2): (2002) 145-153.
6) W. Gille. Wave Random Media 12 (1): (2002) 85-97.
7) B. Smarsly, M. Antonietti, T. Wolff. J. Chem. Phys. 116 (6): (2002) 2618-2627.
8) W. Gille, D. Enke, F. Janowski. J. Porous Mat. 8 (2): (2001) 111-117.
9) J.B.W. Webber, J.H. Strange and J.C. Dore. Magn. Reson. Imaging. 19 (2001) 595.
10) J.B.W. Webber. PhD, Thesis, University of Kent, 2000. http://www.kent.ac.uk/physical-sciences/publications/theses/jbww.html
11) C.L. Jackson and G.B. McKenna. J. Chem. Phys., 93 (1990) 9002.
12) M. Brun, A. Lallemand, J-F. Quinson, and C. Eyraud. Thermochimica Acta, 21 (1977) 59.
13) J.H. Strange, M. Rahman and E.G. Smith, Physical Review Letters, 71 (1993) 3589.
14) J.H. Strange and J.B.W. Webber. Meas. Sci. Technology. 8 (1997) 555.
15) J.B.W.Webber. 6th International Conference on Magnetic Resonance in Porous Media, Ulm, Germany, (2002), Magn. Reson. Imaging 21 (3-4) (2003) 428.
16) J.H. Strange, J. Mitchell and J.B.W. Webber, 6th International Conference on Magnetic Resonance in Porous Media, Ulm, Germany, (2002). Magn. Reson. Imaging 21 (3-4) (2003) 221-226.
17) F. Stepanek, M. Kubicek, M. Marek, P.M. Adler, '*Computer Aided Process Engineering*' - 10 (S. Pierucci, ed.), Elsevier Science, Amsterdam, (2000) 667-672.
18) P. Levitz, Abstr. Pap. Am. Chem. S 223 Part 2 (2002) 211-Phys.
19) E. Hoinkis p. 71 '*Chemistry and Physics of Carbon*' Vol. 25 (2000).
20) N.A. Seaton, J.R.P.B. Walton and N. Quirke, Carbon 27 (1989) 853.
21) M.A. Gardner, PhD Thesis, University of Kent, (1995).
22) A. Szczgielska, A. Burian and J.C. Dore, J. Phys Condensed Matter, 13 (2001) 5545.
23) A. Burien and J.C. Dore, Acta Polonica A, 98 (2000) 457.
24) S.H. Joo, R. Ryoo, M. Kruk and M. Jaroniec, J. Phys Chem B 10 (2002) 4640.
25) J. Dore, Chem. Phys 258 (2000) 327.
26) G. Findenegg, Phys Chem Chem Phys 3 (2001) 1185.
27) S.G. Allen, P.C. Stephenson and J.H. Strange. J. Chem. Phys. 106 18 (1997) 7802.
28) S.G. Allen, P.C. M.J.D. Mallett and J.H. Strange. J. Chem. Phys. 114 7 (2001) 3258.
29) J.C. Dore, J. Baker, P. Behrens and C. Haggenmuller, J. Phys. Chem. B101 (1997) 6226.
30) John Dore, Beau Webber, Monika Hartl, Peter Behrens and Thomas Hansen. Physica A, 314 (2002) 501.
31) H. Farman et al., J. Mol. Liq. 96 (2002) 353.
32) H.F. Booth and J.H. Strange, Magnetic Resonance Imaging 16 5/6 (1998)501.
33) S.G. Allen, P.C. Stephenson and J.H. Strange. J. Chem. Phys. 108 19 (1998) 8195.
34) J.A. Duffy and M.A. Alam, Langmuir 16 (2000) 9513.
35) J. Jaklovsky, `*NMR Imaging, A Comprehensive Bibliography*', Addison-Wesley, Massachusetts, (1983).
36) K. Kaneko, personal communication and E. Bekyarova et al Chem. Phys. Letts. 366 (2002) 463.
37) X.C. Zeng, personal communication, 2003 and J. Bai et al J. Chem. Phys. 118 (2003) 3913.
38) I. Mamina et al, J.Phys Soc Japan **77** 2863 (2002).
39) J.C. Dore, A. Burian and K. Kaneko, allocated beam time for pulsed neutron measurements of ice in carbon nanohorns on GEM/ISIS, 2003.

Figures :

Fig.1a. NMR signal amplitude from the melting cyclohexane in 100Å sol-gel silica.

Fig.1b. Corresponding pore diameter distribution calculated using the Gibbs-Thomson equation.

Fig.2. Co-linearity of melting point depression in water, measured by NMR, compared with gas adsorption pore diameter, for ten sol-gel silicas of pore diameter 25Å - 500Å.

Fig.3. Macroscopic distribution of nanostructure for four tubes containing 40Å, 60Å, 140Å and 200Å pore diameter sol-gel silica.

Fig.4. Combined neutron diffraction and small angle scattering data for seven sol-gel silicas.

Fig.5. Measured solid-solid radial distribution functions *G(r)* for seven sol-gel silicas calculated from SANS data, compared with calculated *G(r)* for models with extended structures of randomised pores.

Fig.6a. USAXS, SAXS and pulsed neutron diffraction on a BP-71 carbon.

Fig.6b. The $d(r) = r.G(r)$ function for the data shown in Fig 6a.

Fig.7. Neutron diffraction at different temperatures for D_2O water/ice in mesoporous SBA-15 (see text for details).

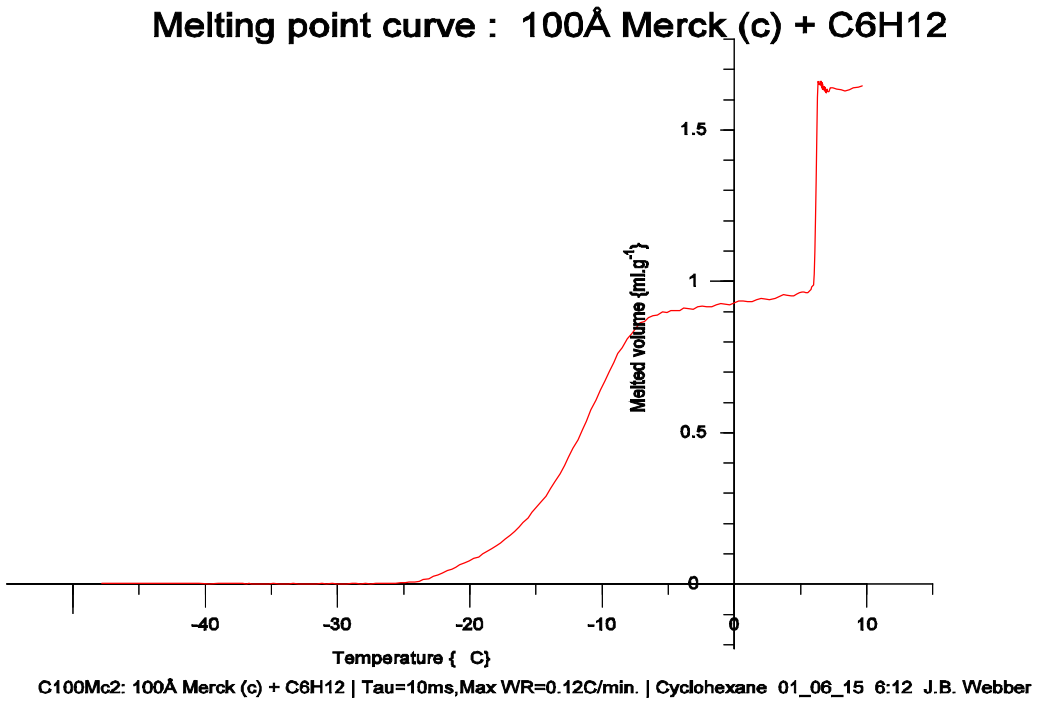

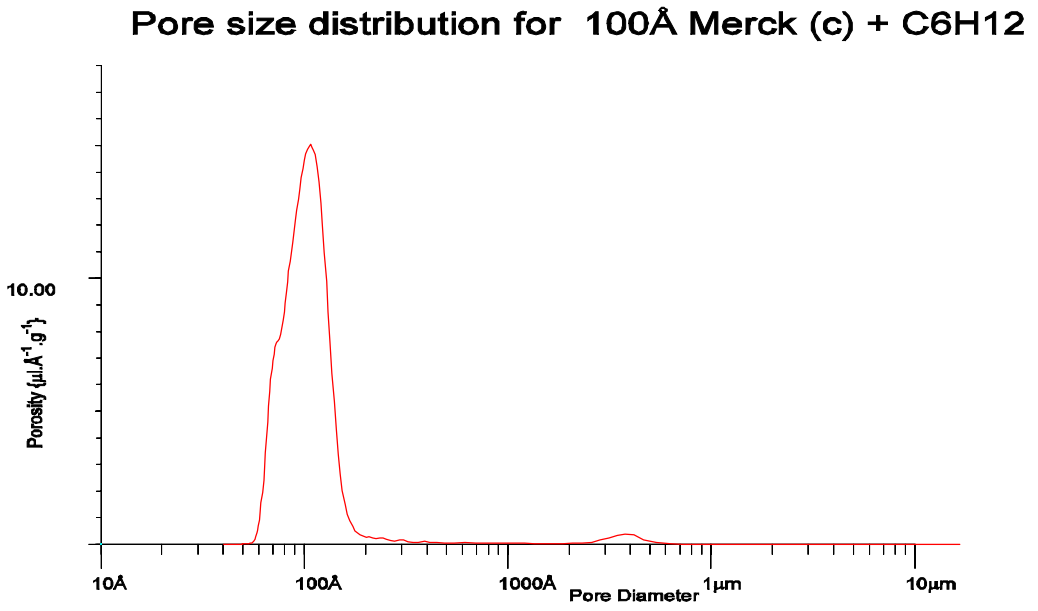

Fig.1a. NMR signal amplitude from the melting cyclohexane in 100Å sol-gel silica.
Fig.1b. Corresponding pore diameter distribution calculated using the Gibbs-Thomson equation.

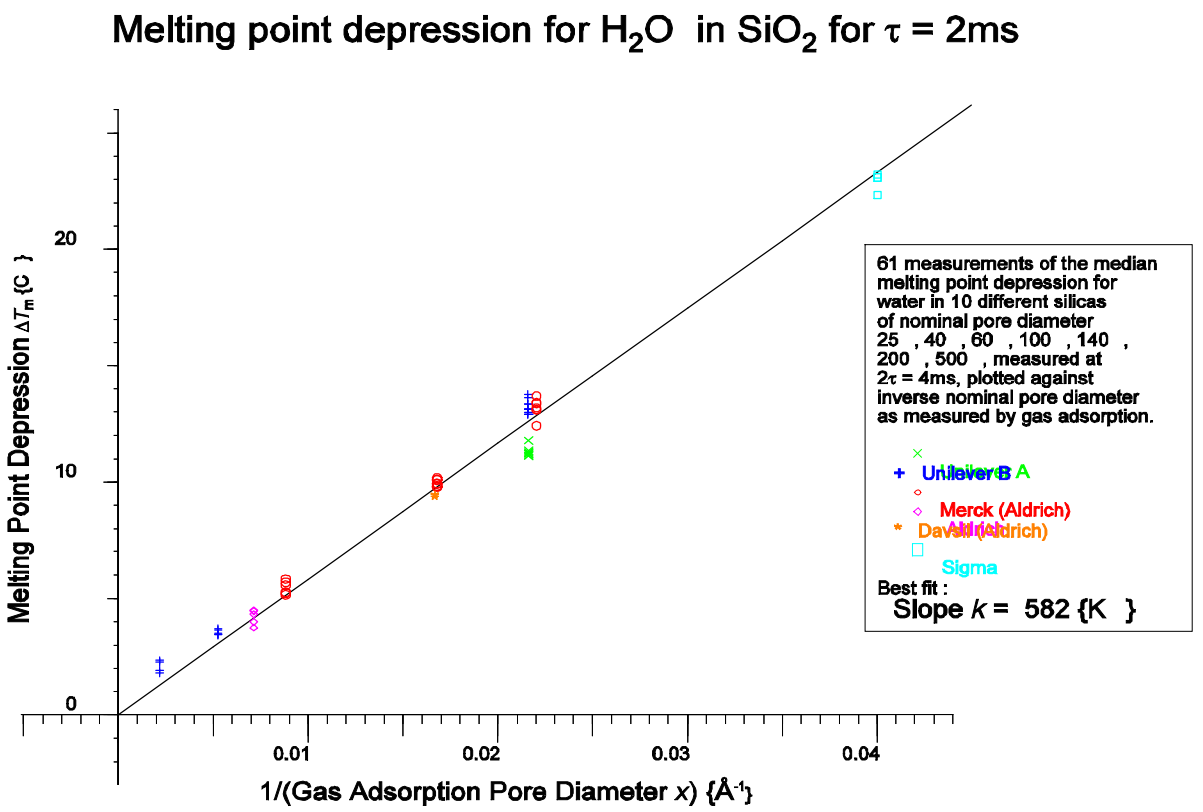

Fig.2. Co-linearity of melting point depression in water, measured by NMR, compared with gas adsorption pore diameter, for ten sol-gel silicas of pore diameter 25Å - 500Å.

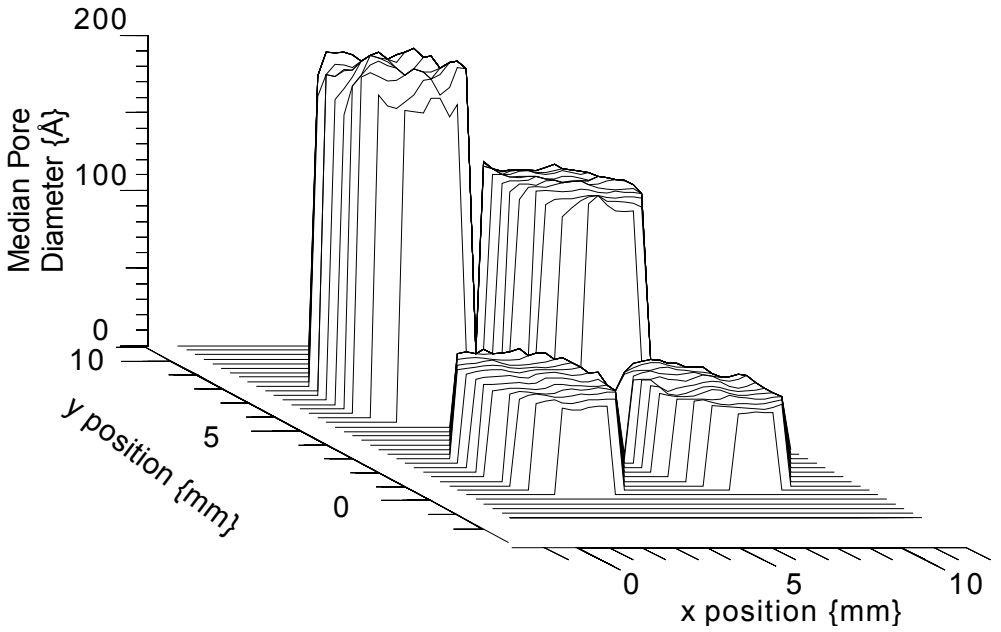

Fig.3. Macroscopic distribution of nanostructure for four tubes containing 40Å, 60Å, 140Å and 200Å pore diameter sol-gel silica.

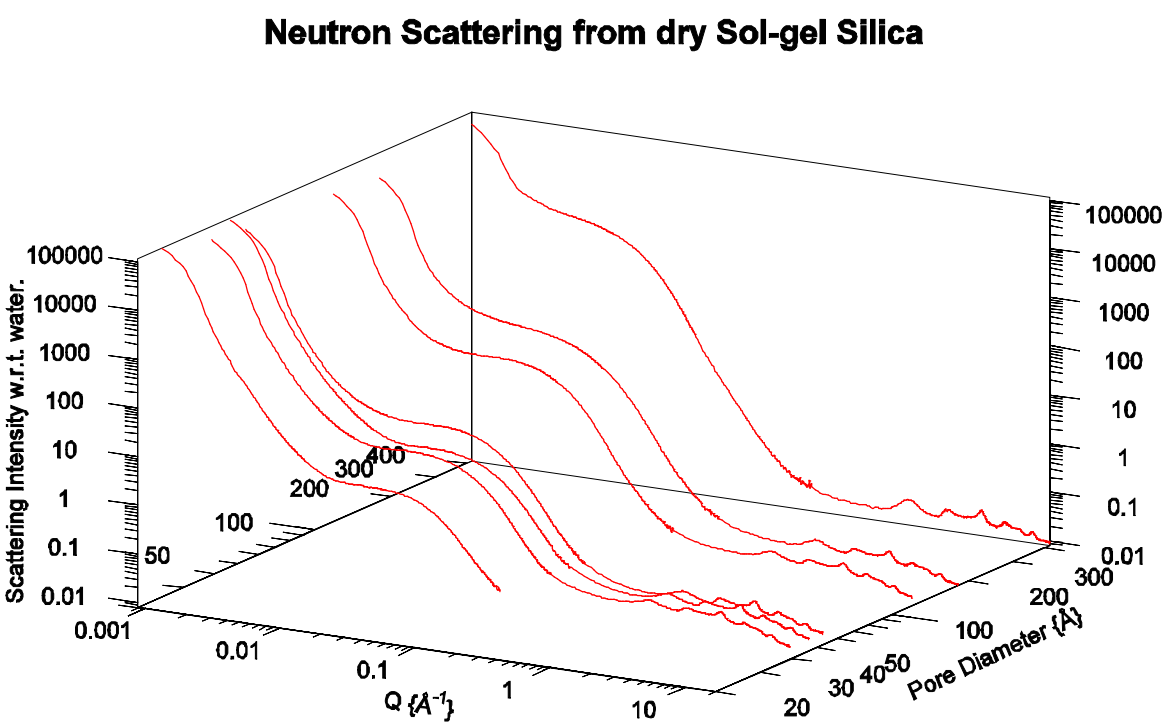

Fig.4. Combined neutron diffraction and small angle scattering data for seven sol-gel silicas.

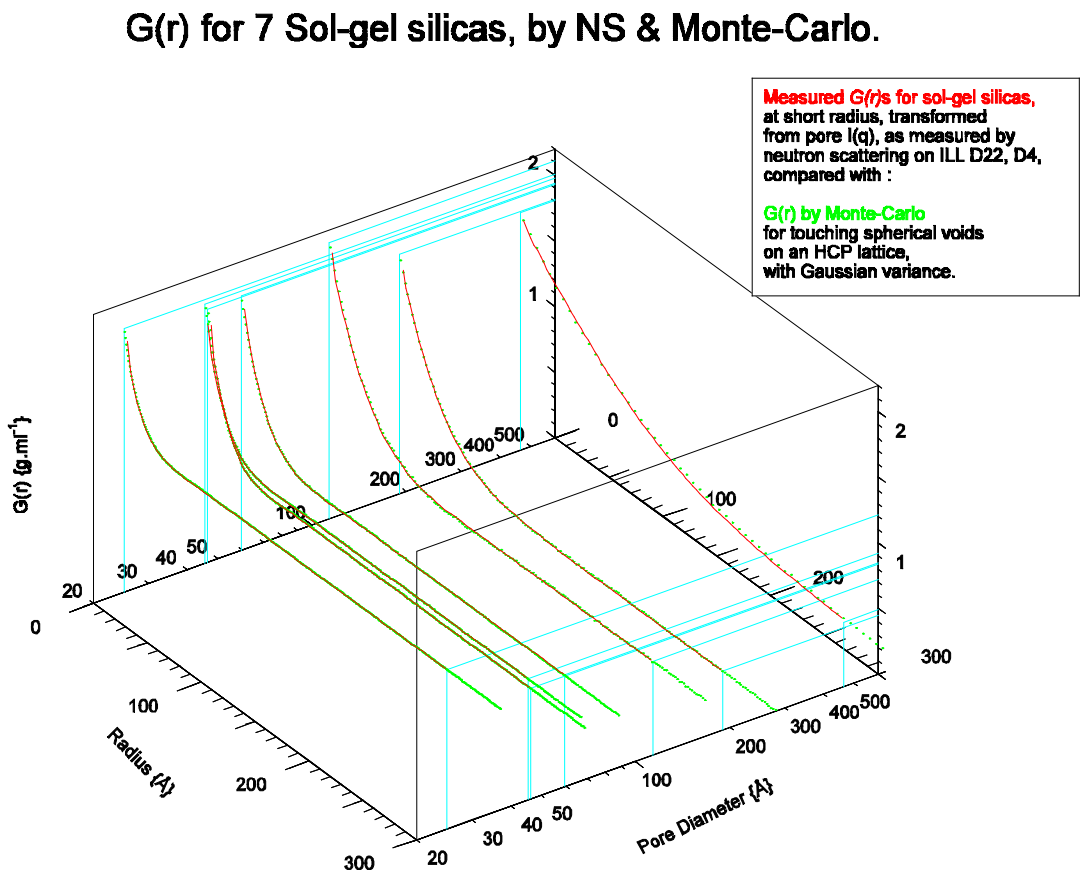

Fig.5. Measured solid-solid radial distribution functions G(r) (lines) for seven sol-gel silicas calculated from SANS data, compared with calculated G(r) (dots) for models with extended structures of randomised pores.

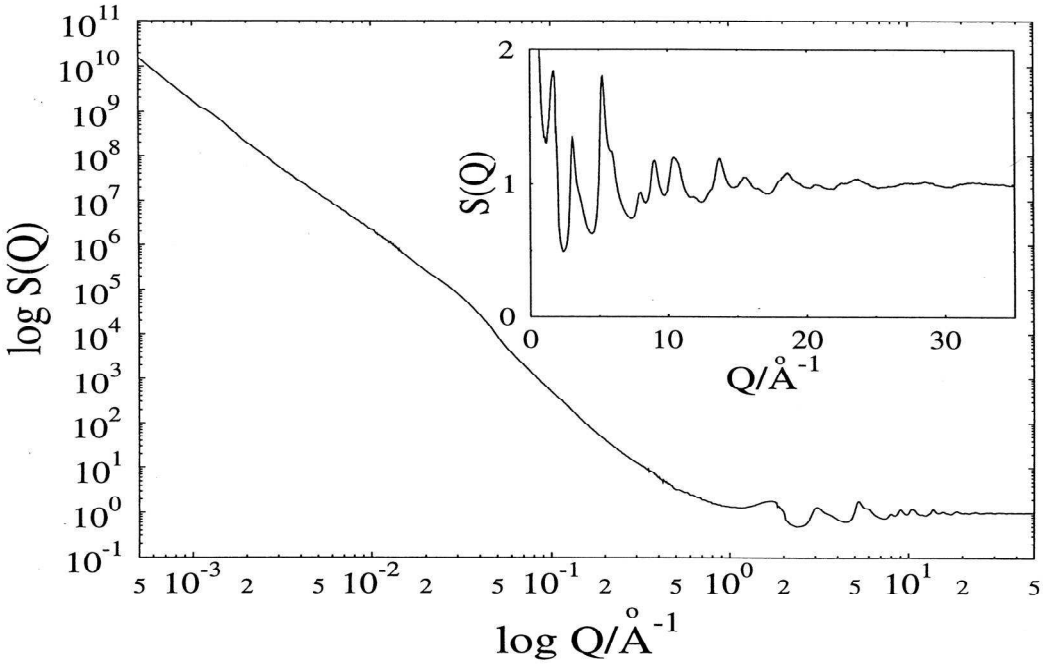

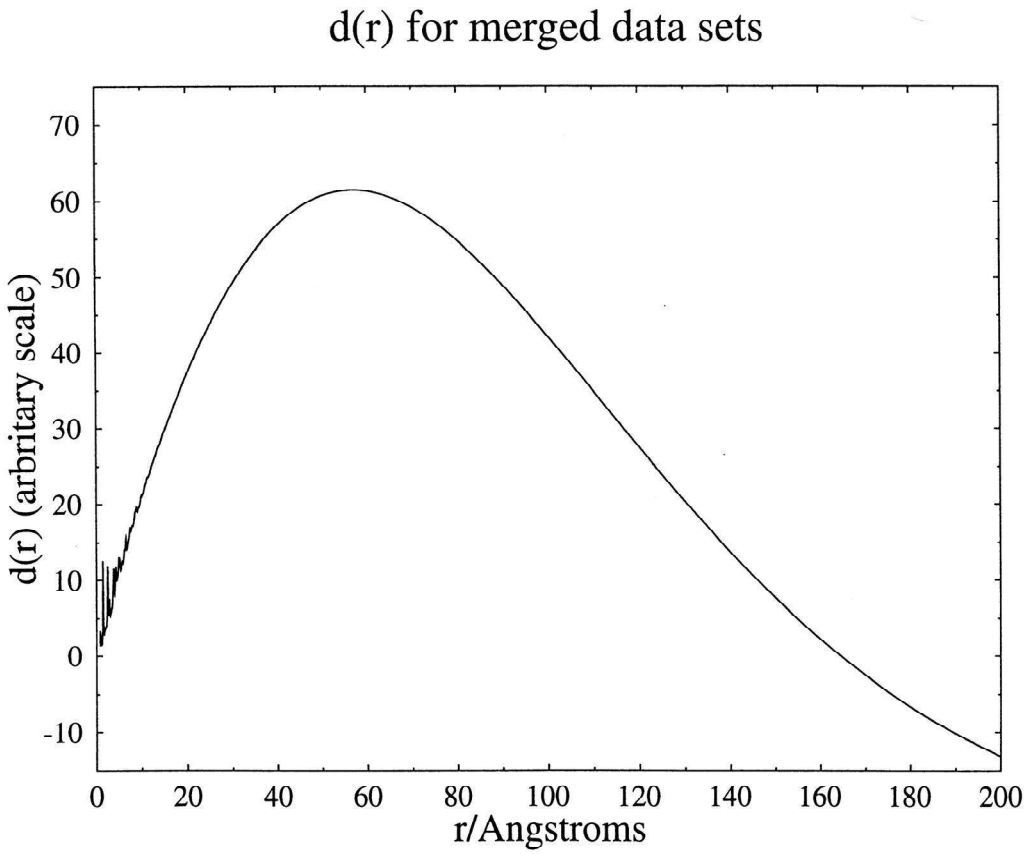

Fig.6a. USAXS, SAXS and pulsed neutron diffraction on a BP-71 carbon.
Fig.6b. The *d(r) = r.G(r)* function for the data shown in Fig.6a.

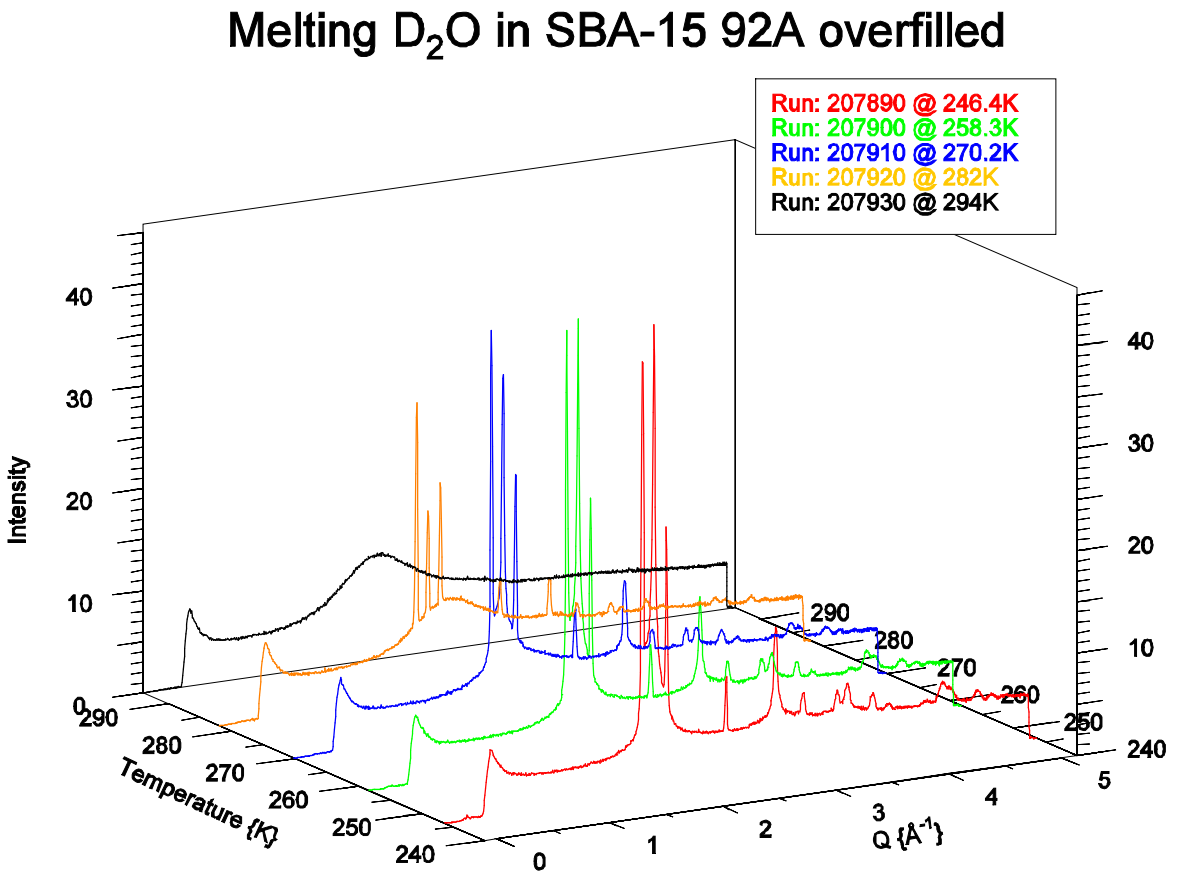

Fig.7. Neutron diffraction at different temperatures for D_2O water/ice in mesoporous SBA-15 (see text for details).